Polymeric Nanocomposite – Based Herbicide of Carboxymethyl Cellulose Coated – Zinc/Aluminium Layered Double Hydroxide – Quinclorac: A Controlled Release Purpose for Agrochemicals

by Rahadian Zainul Et.al

ORIGINAL PAPER

Polymeric Nanocomposite-Based Herbicide of Carboxymethyl Cellulose Coated-Zinc/Aluminium Layered Double Hydroxide-Quinclorac: A Controlled Release Purpose for Agrochemicals

Sharifah Norain Mohd Sharif[1] · Norhayati Hashim[1,2] · Illyas Md Isa[1,2] · Suriani Abu Bakar[3] · Mohamad Idris Saidin[1] · Mohamad Syahrizal Ahmad[1] · Mazidah Mamat[4] · Mohd Zobir Hussein[5] · Rahadian Zainul[6]

Abstract
In this work, the use of carboxymethyl cellulose (CMC) is highlighted in enhancing the controlled release behaviour of zinc/aluminium layered double hydroxide-quinclorac (Zn/Al-LDH-QC). The Zn/Al-LDH-QC-CMC nanocomposite were characterised using powder x-ray diffraction, Fourier transform infrared spectroscopy, thermogravimetric and derivative thermogravimetric analysis and field emission scanning electron microscopy. The release study was carried out in an aqueous solution of Na_3PO_4, Na_2SO_4 and $NaCl$, so as to mimic the environmental condition where the QC is frequently used. The Zn/Al-LDH-QC-CMC nanocomposites showed better performance in releasing QC, with prolonged release time ranging from 163–6083 min, compared to 99–2639 min for the uncoated nanocomposites. The hygroscopic nature of the CMC play a critical role in enhancing the release behaviour of the Zn/Al-LDH-QC-CMC. The kinetic study shows that the Zn/Al-LDH-QC-CMC follows the pseudo-second order kinetic model; hence the release mechanism occurred via dissolution of the CMC matrix and the ion exchange process. These results, therefore, indicate the potential of Zn/Al-LDH-QC-CMC in dealing with the downside effect of the excessive usage of herbicide in paddy cultivation.

✉ Norhayati Hashim
norhayati.hashim@fsmt.upsi.edu.my

[1] Department of Chemistry, Faculty of Science and Mathematics, Universiti Pendidikan Sultan Idris, 35900 Tanjong Malim, Perak, Malaysia

[2] Nanotechnology Research Centre, Faculty of Science and Mathematics, Universiti Pendidikan Sultan Idris, 35900 Tanjong Malim, Perak, Malaysia

[3] Department of Physics, Faculty of Science and Mathematics, Universiti Pendidikan Sultan Idris, 35900 Tanjong Malim, Perak, Malaysia

[4] School of Fundamental Science, Universiti Malaysia Terengganu, 21030 Kuala Terengganu, , Terengganu, Malaysia

[5] Materials Synthesis and Characterization Laboratory, Institute of Advanced Technology, Universiti Putra Malaysia, 43400 Serdang, Selangor, Malaysia

[6] Department of Chemistry, Faculty of Mathematics and Natural Science, Universitas Negeri Padang, Padang, West Sumatera 25171, Indonesia
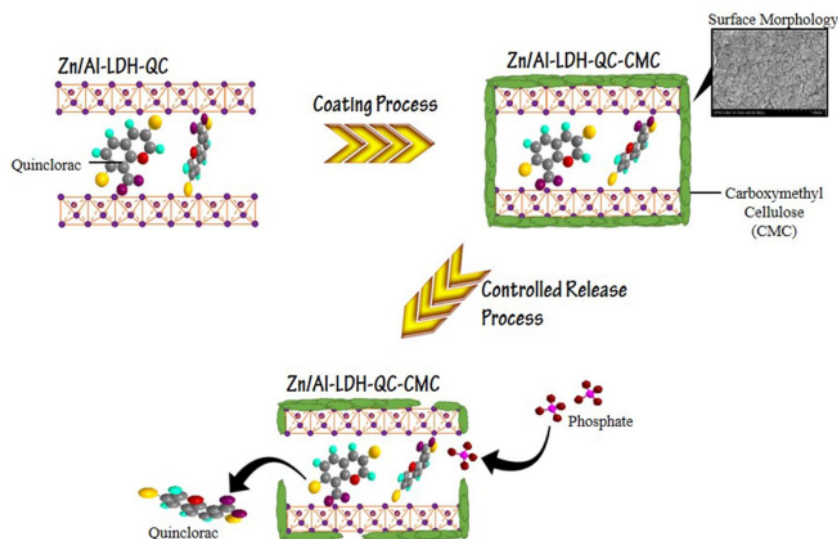
🖄 Springer

Graphic abstract

Introduction

The implementation of controlled release formulation (CRF) in herbicides has long been recognised as an approach to reduce pollution caused by excessive usage of herbicide in the agricultural sector [1–3]. Intercalation of herbicide into suitable host matrix is always a vital key to sustain the release of herbicide into the environment [4–6]. Owing to the interaction between the host matrix and the intercalated herbicide, only a small amount of the herbicide will be released to the environment at a particular time. This would allow the prolonging of the time of the release of herbicide from the host matrix, hence lowering the risk of the environmental pollution. Layered materials, especially layered double hydroxide (LDH) and layered hydroxide salts (LHS) are considered as attractive materials to be used as a host matrix in synthesising a composite with CRF characteristics [5, 7, 8]. The versatility of these layered materials also allowing them to be exploited in various fields including agricultural, pharmaceutical, aesthetic, food processing and sensor technology [9–14].

The potential of a layered material as a host matrix in slowing the release of the herbicide to the environment can be enhanced by coating the intercalated layered material composite with a suitable coater. The coating process generates an additional layer on the outer surface of the composite, hence extending the shelf life of the composite by slowing the herbicide release via controlled diffusion process [15]. The coater will also act as a barrier to protect the composite from unfavourable conditions, including unnecessary moisture, light, and oxygen. Several materials that have shown great potential to be used as a coater may include carboxymethyl chitosan, polymerized octadecylsiloxane, beeswax, chitosan, cellulose, alginate, whey protein, pectin, gelatin and polymers [3, 16–28].

Carboxylmethyl cellulose (CMC), is an anionic, water-soluble cellulose derivative containing many carboxyl and hydroxyl groups in its structure [29]. CMC has attracted much attention owing to its interesting properties, such as high viscosity, transparency, hydrophilicity, non-toxic, biocompatibility, biodegradability, and good film-forming ability [29–37]. The cellulose derivative has been employed in many applications, including in controlled release formulation of herbicide [27, 38, 39]. The chemical structure of carboxymethyl cellulose was shown in Fig. 1.

In this research, we aim to explore further the possibility of using the polysaccharide coating to enhance the CRF applications of a nanocomposite. The Zn/Al-layered double hydroxide-quinclorac nanocomposite (Zn/Al-LDH-QC) was coated with CMC using the direct reaction method, so as to synthesise the CMC coated Zn/Al-LDH-QC nanocomposite (Zn/Al-LDH-QC-CMC).

Fig. 1 The chemical structure of carboxymethyl cellulose
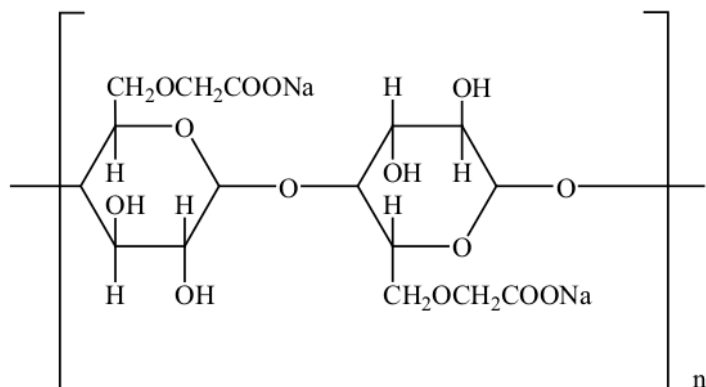
The physicochemical properties of the Zn/Al-LDH-QC-CMC were studied using several instruments and were compared to the physicochemical properties of the Zn/Al-LDH-QC nanocomposite, to thoroughly observe for changes. The study on the controlled release behaviour of the uncoated and coated nanocomposite was conducted in various salt solutions. Obtained results were compared so that the impact of CMC as the coater toward the controlled release properties of the nanocomposite can be investigated. To the best of our knowledge, no previous studies have reported on the uses of CMC coating to enhance the controlled release behaviours of the Zn/Al-LDH-QC nanocomposite.

Experimental

Reagents

All reagents used in this study were purchased from several different suppliers and were used as received. No further purification was performed on any of the reagents. The CMC powder that was used as the coater was obtained from Sigma Aldrich. The main reagents used to synthesised the Zn/Al-LDH-QC nanocomposite, $Zn(NO_3)_2 \bullet 6H_2O$ (98% purity) and $Al(NO_3)_3 \bullet 9H_2O$ (98% purity) were both obtained from Systerm. The intercalated herbicide, QC was supplied from China, with 95% purity. The sodium phosphate, Na_3PO_4 (99.5% purity), sodium sulphate, Na_2SO_4 (95.2% purity) and sodium chloride, NaCl (99.0% purity) were all purchased from Systerm. Deionised water was used as the solvent to prepare all solutions required in the study.

Synthesis of Zn/Al-LDH-QC-CMC Nanocomposite

The Zn/Al-LDH and Zn/Al-LDH-QC nanocomposite was initially synthesised using co-precipitation method, as reported in our previous paper [40]. Zinc nitrate and aluminium nitrate were used as precursors, with a Zn/Al molar ratio, R = 3. The pH was then adjusted until pH 7.5 ± 0.05, by the addition of 2 M NaOH and 1.0 M HCl. In order to coat the synthesised Zn/Al-LDH-QC, 0.1 g of CMC is dissolved in 50 mL of deionised water at room temperature. Once the CMC is completely dissolved, 0.1 g of Zn/Al-LDH-QC nanocomposite was added into the mixture and left for 18 h under constant stirring. The precipitate was collected by centrifuging the mixture for five minutes at 4000 rpm. The product was dried in an oven (70 °C) for 24 h and ground into fine powder before they were kept in a vial for further characterisation and control release study. The whole procedures were repeated to the Zn/Al-LDH in order to prepare the Zn/Al-LDH-CMC.

Characterisation of Zn/Al-LDH-QC-CMC Nanocomposite

The powder x-ray diffraction (PXRD) patterns were recorded using PANalytical X-pert Pro MPD diffractometer. The Co K-alpha radiation was applied at 30 mA and 40 kV (0.15406 nm). Each sample was measured in the range of 2–60° with step size and scan step time of 0.0330° and 19.4434 s, respectively. The Fourier transform infrared (FTIR) spectra were obtained at room temperature on a Nicolet FTIR spectrometer in the KBr phase within the wavenumber range of 400–4000 cm^{-1} and a nominal resolution of 4 cm^{-1}. The thermogravimetric analysis and derivative thermogravimetric analysis (TGA/DTG) of the samples were recorded on a Perkin–Elmer Pyris 1 TGA Thermo Balance at a heating rate of 10 °C min^{-1} in the presence of N_2 gas in the temperature range of 35–1000

°C. The morphology observation was performed using FESEM model Hitachi SU 8020 UHR instrument.

Controlled Release Formulation Study of Zn/Al-LDH-QC-CMC Nanocomposite

The controlled release study was performed using Perkin Elmer ultraviolet–visible (UV–vis) spectrometer, with experimental conditions of λ_{max} = 238.1 nm, time interval = 60 s, slit width = 1.0 nm, lamp change = 326.0 nm, ordinate max = 1.0 and ordinate min = 0.0. The controlled release study was performed in single, binary and ternary system of aqueous solutions, using Na_3PO_4, Na_2SO_4, and NaCl. Each single system aqueous solution was prepared in a series of concentration, ranging from 0.3 M to 1.0 M, whereas the binary and ternary systems of aqueous solution were prepared using 1.0 M aqueous solutions, of several anions combinations. 0.6 mg of Zn/Al-LDH-QC-CMC nanocomposite was then added into a cuvette containing 3.5 mL of the salt solutions, in which the salt solutions were used as a release media for the controlled release study of Zn/Al-LDH-QC-CMC nanocomposite. The cuvette was closed and left in the UV–vis spectrometer until the maximum release of QC was observed.

Results and Discussion

PXRD Analysis

Powder X-ray diffractometry is a useful method in determining whether the CMC coating process does affect the type of ions that were intercalated in the interlayer gallery of the Zn/Al-LDH and Zn/Al-LDH-QC nanocomposite. The determination was made based on the value of basal spacing owned by the peaks of each sample. The result obtained from the PXRD analysis is illustrated in Fig. 2.

In the PXRD pattern of the CMC, no sharp peaks appear, thus reflecting the amorphous structure possessed by the CMC [41]. The PXRD pattern of the Zn/Al-LDH (Fig. 2b) demonstrates reflections at the basal spacing of typical of Zn/Al-LDH, as three diffraction peaks at 10.1°, 20.1°, and 34.1° with the basal spacing values of 8.8 Å, 4.4 Å and 2.4 Å, respectively [42]. The intense, sharp, and symmetrical series of peaks observed in the PXRD pattern of the Zn/Al-LDH thus indicates its good crystallinity. After the Zn/Al-LDH was coated with CMC, these three peaks still emerged and were only slightly shifted (Fig. 2c). The three peaks appear at 11.3°, 23.2°, and 34.3°, with the basal spacing values of 8.1 Å, 4.4 Å and 2.6 Å, respectively. The appearance of peaks with a basal spacing of 8.8 Å in the PXRD pattern of Zn/Al-LDH and 8.1 Å in the PXRD pattern of Zn/Al-LDH-CMC indicates that the nitrate ions remained in
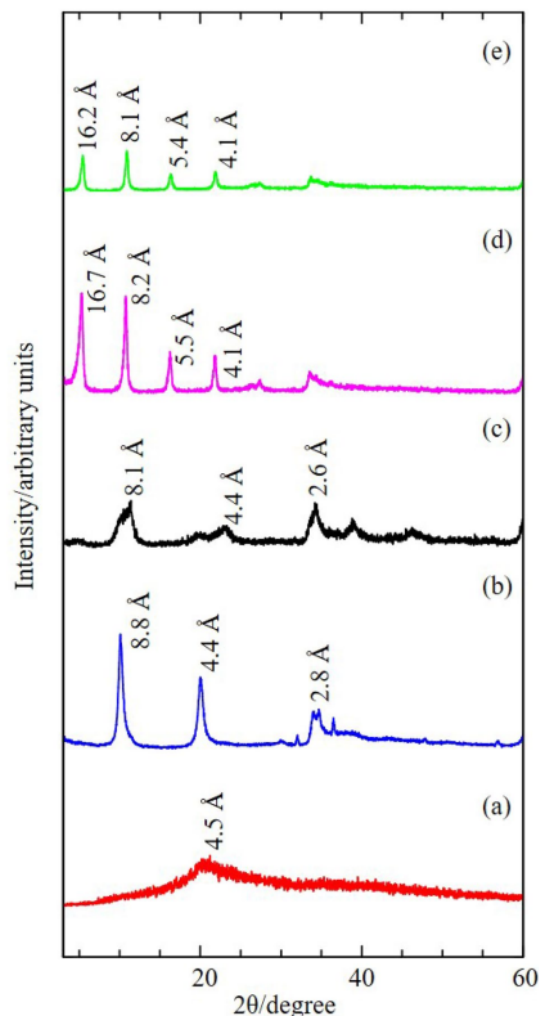

Fig. 2 PXRD patterns of **a** CMC **b** Zn/Al-LDH [40], **c** Zn/Al-LDH-CMC, **d** Zn/Al-LDH-QC [40] and **e** Zn/Al-LDH-QC-CMC

the interlayer gallery of Zn/Al-LDH even after the coating process took place [43]. The PXRD pattern also reveals that the peaks from the coated tend to be broad, asymmetrical, and have lower intensity compared to the uncoated Zn/Al-LDH, thus reflecting the poor crystalline nature possessed by the Zn/Al-LDH-CMC. The disordered layered structure possessed by the Zn/Al-LDH-CMC, therefore, signifies the existence of an amorphous structure of CMC [41].

Figure 2c, d show the PXRD patterns of Zn/Al-LDH-QC before and after it was coated with CMC. Four diffraction peaks were observed in the PXRD pattern of Zn/Al-LDH-QC and Zn/Al-LDH-QC-CMC; as expected, the basal spacing values of the peaks in both samples only slightly differ

from each other. The diffraction peaks in the PXRD pattern of uncoated Zn/Al-LDH-QC appear at 5.3°, 10.7°, 16.3°, and 21.9°, with the basal spacing values of 16.7 Å, 8.2 Å, 5.5 Å and 4.1 Å, respectively. In the PXRD pattern of Zn/Al-LDH-QC-CMC, the peaks emerge at 5.4°, 10.9°, 16.4°, and 21.9°, with the basal spacing values of 16.2 Å, 8.1 Å, 5.4 Å and 4.1 Å, respectively. Although the peak positions in the PXRD pattern of Zn/Al-LDH-QC and Zn/Al-LDH-QC-CMC are only slightly shifted, the coating process did lower the intensity of each peak, thus indicating that there is some reduction in the crystallinity of Zn/Al-LDH-CMC, which is affected by the amorphous nature of the CMC [41]. The appearance of peaks at the lower 2θ angle (at 5.4° in the PXRD pattern of Zn/Al-LDH-QC and at 5.3° in the PXRD pattern of Zn/Al-LDH-QC-CMC) signifies the enlargement of basal spacing due to the intercalation of QC in the interlayer gallery of both Zn/Al-LDH and Zn/Al-LDH-QC [40]. It can be seen that both uncoated and CMC coated Zn/Al-LDH-QC seems to share similar trends as exhibited by the coated and uncoated Zn/Al-LDH, which indicates that the coating process did not cause any alteration concerning the type of the intercalated anion in the interlayer gallery. Therefore, the QC is believed to still be intercalated in the interlayer gallery of Zn/Al-LDH-QC after the CMC coating process [43].

Minor changes to the peak positions in the PXRD patterns of both Zn/Al-LDH and Zn/Al-LDH-QC before and after they undergo the coating process are due to the fact that CMC coater was only adsorbed on the outer surface of Zn/Al-LDH and Zn/Al-LDH-QC and did not replace the existing anions in the interlayer gallery of both Zn/Al-LDH and Zn/Al-LDH-QC [43]. The anionic polymeric chain like CMC may be combined with the Zn/Al-LDH via several manners. It is possible for the polymeric chain to be intercalated into the interlayer gallery of Zn/Al-LDH, which would result in a major expansion of the interlayer spacing [44]. Recent studies also have reported on that the combination of Zn/Al-LDH and the polymeric chain forms an exfoliated nanocomposite, where the stacked layers of Zn/Al-LDH are fully separated. The exfoliation allows each layer to be functionalised with the polymeric chain [45, 46]. However, in the case of this study, the PXRD analysis has shown that the CMC is associated with the Zn/Al-LDH and Zn/Al-LDH-QC by aggregation, which is proven by a minute or non-existent expansion of their interlayer galleries after undergoing the coating process [43]. The schematic representation of the aggregation type of Zn/Al-LDH-QC-CMC produced from the interaction between the Zn/Al-LDH-QC nanocomposite and CMC is shown in Fig. 3.

The PXRD patterns also reveal that the peaks that indicate the turbostratic effect (represented by the formation of saw–toothed peaks located at 33°) in both PXRD patterns of the Zn/Al-LDH and Zn/Al-LDH-QC can still be observed
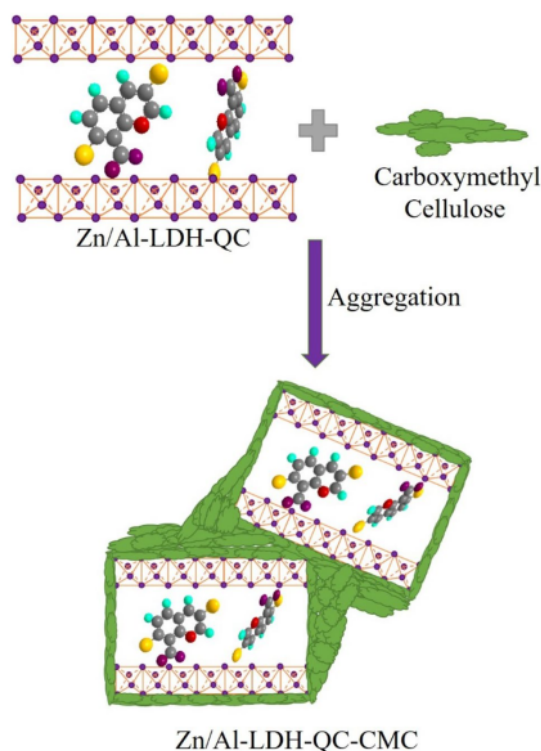

Fig. 3 Schematic representation of the aggregation type of Zn/Al-LDH-QC-CMC produced from the interaction between the Zn/Al-LDH-QC nanocomposite and CMC

after the CMC coating process. Turbostratic effect is commonly associated to a specific morphology, in which the material develops as aggregates of thin crumpled layers with indefinite size, resulting from weak interactions between the interlayer species and the host lattice [47–49]. Hence, the appearance of the turbostratic peaks on the Zn/Al-LDH-CMC and Zn/Al-LDH-QC-CMC prove that the interlayer structure of both nanocomposites remain unchanged after the CMC coating process.

The result obtained from the PXRD analysis, therefore, proves that the coating process using CMC as a coater did not cause any anions to be replaced in the interlayer gallery of Zn/Al-LDH, although there might be some reduction on peak intensity due to the existence of amorphous CMC in Zn/Al-LDH-CMC and Zn/Al-LDH-QC-CMC.

Spatial Arrangement of Carboxymethyl Cellulose Coated Zn/Al-LDH-QC Nanocomposite

The basal spacing values obtained from the PXRD analysis enable the height of the interlayer gallery of the Zn/Al-LDH to be calculated. These basal spacing values indicate that the

intercalated QC was arranged in the interlayer gallery of Zn/Al-LDH as a monolayer and was maintained in that position due to an electrostatic interaction between the positively charged Zn/Al-LDH layer and the negatively charged QC anions [40]. The spatial arrangement was proposed based on the prediction made using Chem 3D Ultra 8.0 software. Even though the PXRD analysis reveals that only minor changes were observed in the basal spacing values after the Zn/Al-LDH-QC underwent the CMC coating process, these changes still induced the interlayer gallery height of the Zn/Al-LDH nanocomposite to be slightly reduced from 11.9 Å to 11.4 Å. This shrinkage was enough to force the QC to be arranged in a more tilted position within the interlayer gallery of Zn/Al-LDH. The proposed spatial arrangement of the uncoated and CMC-coated Zn/Al-LDH-QC is shown in Fig. 4.
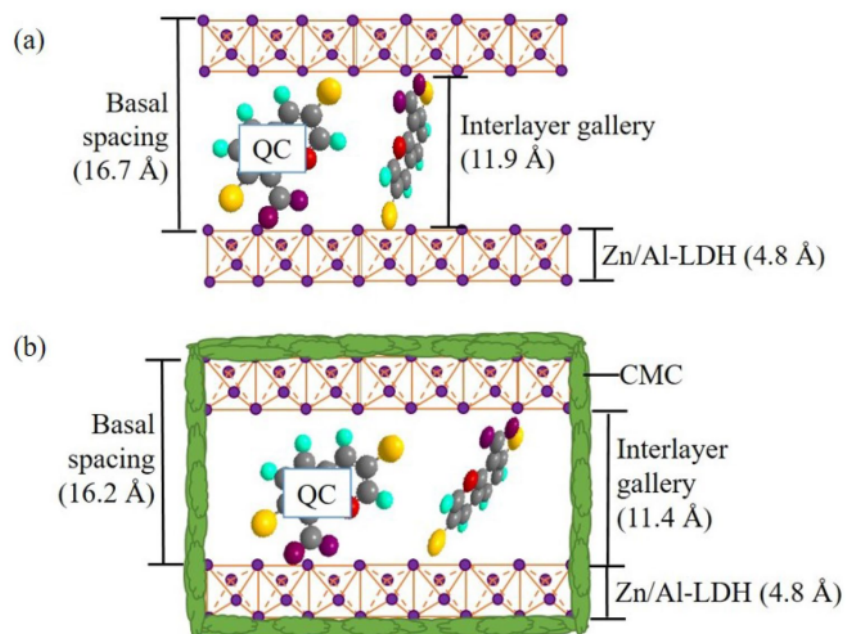
FTIR Analysis

Figure 5 illustrates the corresponding FTIR spectra for Zn/Al-LDH, QC anion, Zn/Al-LDH-QC, CMC, Zn/Al-LDH-CMC and Zn/Al-LDH-QC-CMC in the range of 4000–400 cm^{-1}. The results obtained from the FTIR analysis were also compared with those obtained in previous studies and summarised in Table 1 [40]. A broad peak attributed to the stretching of –OH groups and water molecules is observed in the FTIR spectra of all samples. This peak appears in the FTIR spectra of Zn/Al-LDH, QC anion, Zn/Al-LDH-QC, CMC, Zn/Al-LDH-CMC and Zn/

Al-LDH-QC-CMC at 3450, 3547, 3342, 3512, 3357, and 3333 cm^{-1}, respectively. Hence, all samples contained –OH groups [29].

The peaks related to the symmetrical and asymmetrical stretching vibrations of the carboxylate group can be seen in the FTIR spectrum of CMC at 1618 and 1432 cm^{-1}, respectively [29]. The absorption peak at 1051 cm^{-1} is ascribed to the –C–O– stretching on the polysaccharide skeleton of the CMC. Moreover, the characteristic peaks of CMC seem to appear in the FTIR spectra of both Zn/Al-LDH-CMC and Zn/Al-LDH-QC-CMC. The peaks that signify the symmetrical and asymmentrical stretching vibration of COO$^-$ are found in the FTIR spectrum of Zn/Al-LDH-CMC at 1584 and 1474 cm^{-1}, and also at 1567 and 1478 cm^{-1} in the spectrum of Zn/Al-LDH-QC-CMC. The peaks denoting the –C–O– stretching on the polysaccharide skeleton of the CMC are found in the spectra of Zn/Al-LDH-CMC and Zn/Al-LDH-QC-CMC at 1045 and 1028 cm^{-1}, respectively. The FTIR analysis, therefore, indicates that traces of CMC exist in both Zn/Al-LDH and Zn/Al-LDH-QC-CMC.

The peaks associated to the bending vibration of Al–OH and Zn–Al–OH appear in the FTIR spectrum of Zn/Al-LDH at 604 and 430 cm^{-1}, respectively [50]. Comparable peaks are also observed in the spectrum of Zn/Al-LDH-QC at 512 and 456 cm^{-1}, the Zn/Al-LDH-CMC spectrum at 543 and 416 cm^{-1}, and the Zn/Al-LDH-QC-CMC spectrum at 535 and 427 cm^{-1}. The peak at 1385 cm^{-1} in the Zn/Al-LDH spectrum represents the symmetric stretching of the NO$_3^-$, thus signifying the existence of NO$_3^-$ as the counter ion in

Fig. 4 Spatial arrangement of QC in the interlayer gallery of Zn/Al-LDH **a** before coating with CMC and **b** after coating with CMC
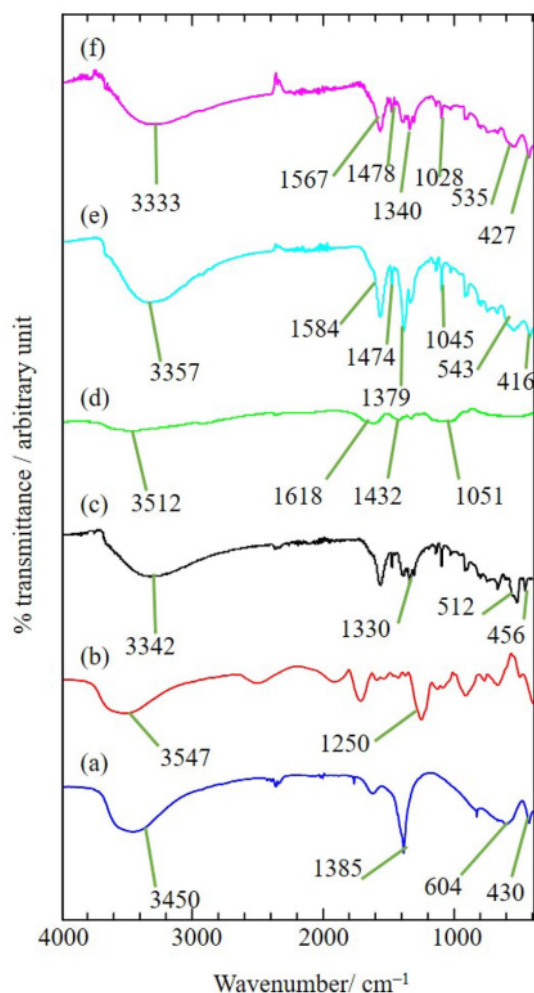
Fig. 5 FTIR spectra **a** Zn/Al-LDH [40] **b** QC anion [40] **c** Zn/Al-LDH-QC [40] **d** CMC **e** Zn/Al-LDH-CMC **f** Zn/Al-LDH-QC-CMC

the interlayer gallery of the Zn/Al-LDH [51]. A similar peak is also detected in the FTIR spectrum of Zn/Al-LDH-CMC at 1379 cm^{-1}. An absorption peak that signifies the presence of a C–N stretching mode in the aromatic moiety of the intercalated QC can be seen in the FTIR spectra of QC, Zn/Al-LDH-QC and Zn/Al-LDH-QC-CMC at 1250, 1330, and 1340 cm^{-1}, respectively [40]. Therefore, it can be suggested that the coating process did not cause any modification on the host or on the intercalated anions; hence, this shows that the FTIR analysis is in good agreement with the PXRD analysis.

Thermal Stability Studies

In order to elucidate the effect of CMC coating process on the thermal behaviour of the Zn/Al-LDH, and Zn/Al-LDH-CMC, thermal stability studies were performed using TGA/DTG in the range of 35–1000 °C. The TGA/DTG curves of the CMC, Zn/Al-LDH-CMC and Zn/Al-LDH-QC-CMC are illustrated in Fig. 6. The maximum temperature in each stage of the thermal decomposition (T_{max}) and its percentage decomposition were compared with recent studies to observe the impact of the CMC coating on thermal stability (Table 2). In the TGA/DTG curve of CMC (Fig. 6a), the thermal decomposition due to the evaporation of water is 9.2% of weight loss upon heating to 220 °C (peak centred at 82.1 °C). Further heating has led to the degradation of CMC at 349.5 °C with 66.2% of weight loss as previously reported [52].

The thermal decomposition of the host Zn/Al-LDH was characterised by three weight loss events. The first thermal decomposition happened at 121.8 °C with 5.5% weight loss, owing to the water removal from the outer surface of Zn/Al-LDH. The second thermal decomposition occurred at 331.0 °C (8.6% weight loss) due to the elimination of the interlayer water molecule; the last stage of the thermal decomposition happened at 251.5 °C (15.3% weight loss) resulting from

Table 1 FTIR Spectra of Zn/Al–LDH, QC, Zn/Al–LDH–QC, Carboxymethyl Cellulose, Zn/Al–LDH–CMC and Zn/Al–LDH–QC–CMC

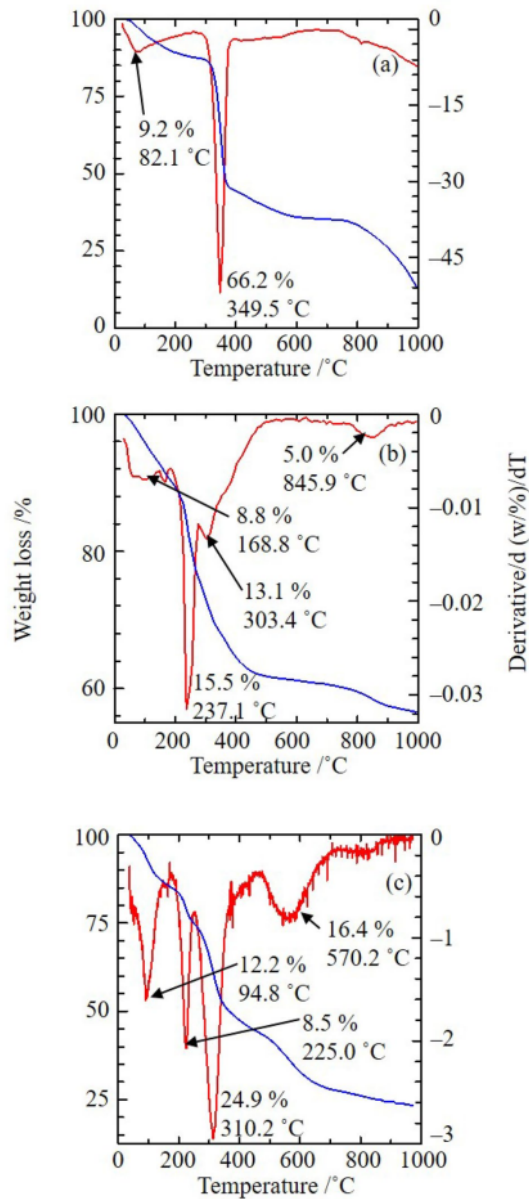| Characteristic group	Zn/Al–LDH	Quinclorac	Zn/Al–LDH–QC	CMC	Zn/Al–LDH–CMC	Zn/Al–LDH–QC–CMC
ν(O–H) in H$_2$O	3450	3547	3342	3512	3357	3333
ν_s(C-N) in amide	–	1250	1330	–	–	1340
ν_s(O–N–O)	1385	–	–	–	1379	–
ν_{as}(COOH)	–	–	–	–	–	–
ν_s(COO$^-$)	–	–	1473	1618	1584	1567
ν_{as}(COO$^-$)	–	–	1564	1432	1474	1468
ν_s(C-O) in polysaccharide skeleton	–	–	–	1051	1045	1028
ν(Zn-Al–OH)	430	–	456	–	416	427
ν(Al–OH)	604	–	512	–	543	535
Ref	[40]	[40]	[40]	Present paper	Present paper	Present paper

Fig. 6 TGA/DTG curves of **a** carboxymethyl cellulose, **b** Zn/Al-LDH-CMC and **c** Zn/Al-LDH-QC-CMC

the dihydroxylation of the Zn/Al-LDH [53]. As for Zn/Al-LDH-CMC, the thermal decomposition progressed through four major steps of weight loss (Fig. 6b), which happened at 168.8 °C (8.8%), 237.1 °C (15.5%), 303.4 °C (13.1%) and 845.9 °C (5.0%). Hence, it was found that the major increment on the maximum thermal decomposition of Zn/

Al-LDH occurred from 303.4 °C to 845.9 °C after it was coated with CMC.

In the case of Zn/Al-LDH-QC, TGA/DTG analysis shows that the thermal decomposition occurred in three stages. The first and the second decompositions are similar to the TGA/DTG curve of Zn/Al-LDH. The first thermal decomposition is due to the removal of the outer surface water molecule, which took place at 97.7 °C (with 9.8% weight loss), whereas the second thermal decomposition is caused by the elimination of the water molecule in the interlayer gallery of the Zn/Al-LDH-QC at 223.5 °C (with 9.2% of weight loss). The last weight loss that occurred at 321.7 °C results from the total decomposition of organic moieties originating from the intercalated QC [40]. After undergoing the CMC coating process, the thermal characteristic of the Zn/Al-LDH-QC-CMC is quite similar to the precursor (Fig. 6c). Four significant weight loss events can be observed in the TGA/DTG curve of Zn/Al-LDH-QC-CMC. The first three stages of the thermal decomposition are comparable with those appearing in the TGA/DTG curve of uncoated Zn/Al-LDH-QC. The first, second and third thermal decompositions occurred at 94.8 °C (12.2%), 225.0 °C (8.5%) and 310.2 °C (24.9%), respectively. The last thermal decomposition at the highest temperature of 570.2 °C resulted in 16.4% weight loss. It was observed that the maximum thermal decomposition of Zn/Al-LDH-QC-CMC at 570.2 °C is much higher compared to Zn/Al-LDH-QC (321.7 °C).

The results obtained from thermal stabilities studies, therefore, show that the trend of the thermal decomposition of Zn/Al-LDH-QC after being coated with CMC was similar to that of Zn/Al-LDH-CMC. This thus indicates that the CMC coating process does enhance the thermal stability of both Zn/Al-LDH and Zn/Al-LDH-QC. These findings were also consistent with those obtained in the recent study that also shows the potential polysaccharide coating in enhancing thermal stability of a material [54, 55].

Surface Morphology Analysis

The surface morphology of pure CMC, Zn/Al-LDH, Zn/Al-LDH-CMC, Zn/Al-LDH-QC and Zn/Al-LDH-QC-CMC is illustrated in Fig. 7. The CMC morphology is observed to be smooth and even. The Zn/Al-LDH morphology is demonstrated as a non-uniform, irregular agglomerate with compact and non-porous plate-like structures, which is expected from typical Zn/Al-LDH samples [43]. The Zn/Al-LDH-QC sample also seems to exhibit irregular plate-like structures but with smaller particle sizes compared to Zn/Al-LDH [40].

It is clear from these images that the Zn/Al-LDH-CMC and Zn/Al-LDH-QC-CMC structures resemble those of the starting precursor, with the main additional morphology after the CMC coating process. The existence of CMC on the Zn/Al-LDH led to the formation of a flaking, uneven

Table 2 TGA/DTG data of weight loss for CMC, Zn/Al-LDH, Zn/Al-LDH-CMC, Zn/Al-LDH-QC and Zn/Al-LDH-QC-CMC

Thermal decomposition		Samples				
		CMC	Zn/Al-LDH	Zn/Al-LDH-CMC	Zn/Al-LDH-QC	Zn/Al-LDH-QC-CMC
Stage 1	T_{max} (°C)	82.1	121.8	168.8	97.7	94.8
	Percentage (%)	9.2	5.5	8.8	9.8	12.2
Stage 2	T_{max} (°C)	349.5	251.5	237.1	223.5	225.0
	Percentage (%)	66.2	15.3	15.5	9.2	8.5
Stage 3	T_{max} (°C)	–	331.0	303.4	321.7	310.2
	Percentage (%)	–	8.6	13.1	22.5	24.9
Stage 4	T_{max} (°C)	–	–	845.9	–	570.2
	Percentage (%)	–	–	5.0	–	16.4
Ref		Present paper	[40]	Present paper	[40]	Present paper

and wrinkly layer that concealed the agglomerate structure of Zn/Al-LDH. As for Zn/Al-LDH-QC, the CMC coating process seems to flatten Zn/Al-LDH-QC, thus causing the tiny plate-like structure of the Zn/Al-LDH-QC-CMC to be more compact than its precursor.

Release Study of Zn/Al-LDH-QC-CMC Nanocomposite into Various Aqueous Solutions

To understand the controlled release behaviour of QC from the Zn/Al-LDH-QC-CMC nanocomposite, the concentration of QC that was released into the single, binary and ternary system of release media was monitored as a function of time. The release study was tested in the aqueous solution of Na_3PO_4, Na_2SO_4, and NaCl. These aqueous solutions were chosen as release media in the study so as to mimic the environmental condition where the intercalated QC is frequently used. The QC is normally used to eliminate the weeds that invade the paddy cultivation area and disrupt the paddy growth, whereas the PO_4^{3-}, SO_4^{2-} and Cl^- are the type of anions that can actually be found in the soil of areas for paddy cultivation [56–67]. Hence, these aqueous solutions of Na_3PO_4, Na_2SO_4, and NaCl were selected as the release media in the study due to their ability to provide the required anions. The results collected from the release study were incorporated into the release profile that is illustrated in Fig. 8.

Generally, the release behaviour of the Zn/Al-LDH-QC-CMC nanocomposite was affected by the type of anions available in the release media during the release process. When the QC was released into the single system of aqueous solutions, the highest percentage release is obtained when the Zn/Al-LDH-QC-CMC nanocomposite is released in the release media containing PO_4^{3-} with 87.3% of maximum

percentage release, followed by Cl^- and SO_4^{2-}, with maximum percentage release of 80.0% and 70.1%, respectively. The highest percentage release achieved when releasing the Zn/Al-LDH-QC-CMC in the aqueous solution of Na_3PO_4, was triggered by the fact that the PO_4^{3-} possess the highest charge density compare to the SO_4^{2-} and Cl^-, thus enhancing the ion exchange process between the intercalated QC and the PO_4^{3-} in the release media [7].

When comparing the release behaviour of QC from the Zn/Al–LDH–QC–CMC in single system of aqueous solution, in term of their time release, the release pattern is generally similar as in the release of the QC from the Zn/Al–LDH–QC–Chi nanocomposite [54]. The slowest release was obtained when using NaCl as the release media, followed by the Na_2SO_4 and Na_3PO_4. The release profile of Zn/Al-LDH-QC-CMC nanocomposite in the NaCl shows that the fast release occurred in the first 0–6083 min (0.3 M), 0–4506 min (0.5 M) and 0–3004 min (1.0 M). The release was then gradually become slower, before its finally reaching equilibrium. When the Na_2SO_4 was used as the release media, the fast release can be seen to happen in the first 0–1436 min (0.3 M), 0–1259 min (0.5 M) and 0–245 min (1.0 M). The release of the intercalated QC from the interlayer gallery of the Zn/Al-LDH-QC-CMC nanocomposite is the fastest when using Na_3PO_4 as the release media. The fast release occurred at first the 0–614 min (0.3 M), 0–480 min (0.5 M) and 0–163 min (1.0 M). The release is significantly prolonged when the nanocomposite was release in the release media containing Cl^- is because the Cl^- is a monovalent anion, hence posssess so much lower affinity towards the positively charged layer of the Zn/Al-LDH than the trivalent PO_4^{3-} and divalent SO_4^{2-} ions [7, 68, 69].

In order to observe the effect of multiple types of incoming ions (provided by the release medium) on the release
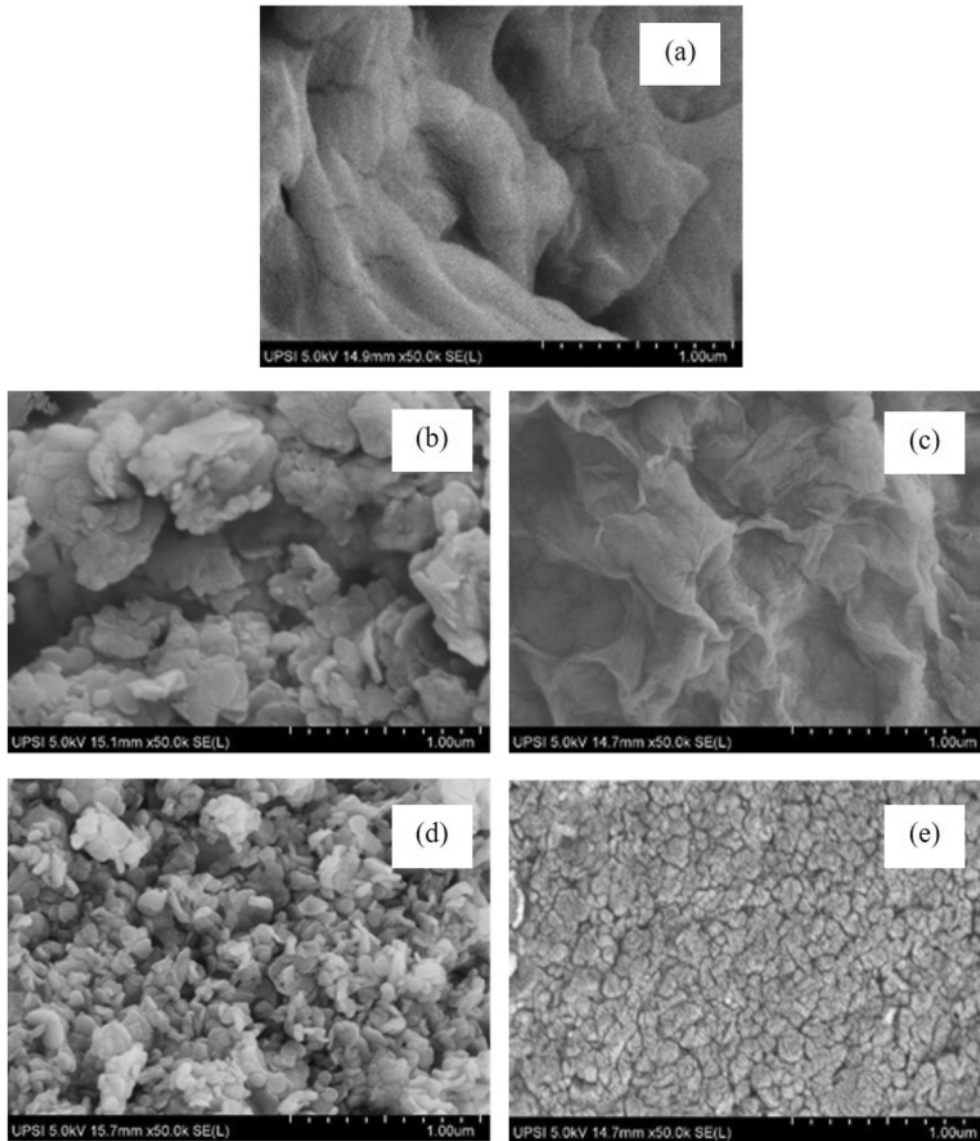
Fig. 7 Surface morphology of **a** carboxymethyl cellulose **b** Zn/Al-LDH [40], **c** Zn/Al-LDH-CMC, **d** Zn/Al-LDH-QC [40] and **e** Zn/Al-LDH-QC-CMC

behaviour of QC from Zn/Al-LDH-QC-CMC, several mixtures of aqueous solutions containing different combinations and compositions of PO_4^{3-}, SO_4^{2-} and Cl^- were used as the release medium in the release study. For the binary anion system, three mixtures of PO_4^{3-}–SO_4^{2-}, PO_4^{3-}–Cl^- and SO_4^{2-}–Cl^- were used. For the ternary anion system, a mixture of PO_4^{3-}–SO_4^{2-}–Cl^- was used as the release medium.

In the release of the QC from Zn/Al–LDH–QC–CMC nanocomposite in aqueous solutions containing multiple type of anions, the results obtained from the study show that the highest percentage of accumulated release and the fastest rate of the release process were observed when the mixtures containing PO_4^{3-}–SO_4^{2-}–Cl^- were used as the release media. The results obtained from the study also show that the highest percentage of accumulated release and the fastest rate of the release process were observed when the mixtures containing PO_4^{3-}–SO_4^{2-}–Cl^- were used as the release medium. As expected, the mixtures
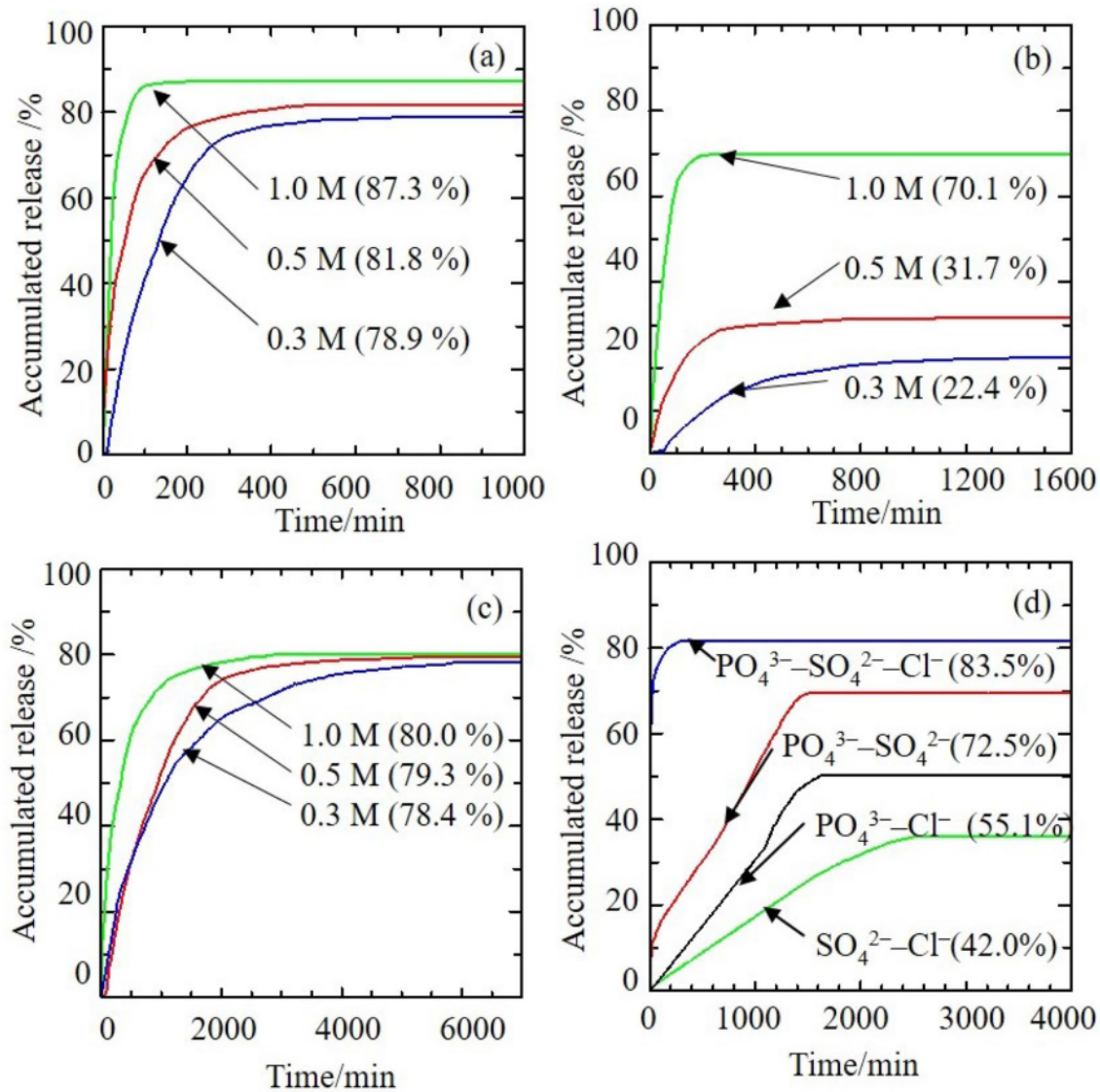
Fig. 8 Release profiles of QC from Zn/Al–LDH–QC–CMC into aqueous solutions of **a** sodium phosphate, **b** sodium sulphate, **c** sodium chloride and **d** phosphate, sulphate and chloride mixture

containing Cl^- anions were found to have a lower percentage of accumulated release and a longer time release. This is mainly contributed to by the monovalent nature of Cl^-, which has a significantly low affinity toward the Zn/Al-LDH layer, therefore making the release process more challenging [7, 68]. The release process of Zn/Al–LDH–QC–CMC in binary and ternary systems of aqueous solutions can be arranged according to their percentage of accumulated release in the order

of $PO_4^{3-}-SO_4^{2-}-Cl^-$ $(83.5\%) > PO_4^{3-}-SO_4^{2-}$ (72.5%) $> PO_4^{3-}-Cl^-$ $(55.1\%) > SO_4^{2-}-Cl^-$ (42.0%).

Generally, the release profile revealed that manipulating the type, concentration and composition of anions in the release medium consequently generated different patterns of release behaviour of the intercalated QC. When the mixtures containing PO_4^{3-} anions were used in the release study, the rate of the release process were found to be faster than in the other release medium. In fact, the percentages of

accumulated release of QC into the release medium were observed to be higher. The dominant influence of PO_4^{3-} anions in increasing the release rate of QC were the result of the multiple hydrolysis processes of the phosphate, which end up leaving the tertiary PO_4^{3-} anions in the mixture [70]. The trivalent PO_4^{3-} anions, which have a high affinity toward the positively charged Zn/Al-LDH layer, were left to compete with the SO_4^{2-} and Cl^- anions, which were acknowledged to have a lower affinity compared to the PO_4^{3-} anions. The comparison made on the accumulated percentage release and time taken for the release of QC from the Zn/Al-LDH-QC, Zn/Al-LDH-QC-Chi (as reported in our recently published paper) and Zn/Al-LDH-QC-CMC to reach equilibrium is summarised in Table 3.

Even though our previous paper revealed that the presence of chitosan has been proven to prolong the release time of QC, the release time seems to be further enhanced when the CMC was used as a coating material. The release time of QC from the Zn/Al–LDH–QC–CMC is so much slower than the release time of QC from the Zn/Al–LDH–QC and Zn/Al–LDH–QC–Chi nanocomposites. Owing to the fact that the CMC is an anionic polysaccharide and the Zn/Al–LDH is a positively charged layered material, the coating process is therefore, generate the formation of strong electrostatic attraction between the positively charged Zn/Al–LDH layer and the negatively charged carboxylate moieties on the CMC chain [29]. As a result of this attraction, more time is needed for the dissolution of the CMC, hence assist in releasing the QC is slower manner. The large swelling capability and high hygroscopic nature possessed by CMC play a critical role

in prolonging the release time of the Zn/Al-LDH-QC [27]. These properties enable the hydrophilic CMC to easily absorb moisture from its surroundings and form a thick gel layer that entrapped the Zn/Al-LDH-QC nanocomposite. As more water molecules were absorbed into the CMC matrix, the gel layer grew and become thicker. A recent study has shown that the release of the particle entrapped in the hydrophilic matrix of CMC can occur via diffusion and the erosion of the CMC gel layer [71].

The results presented up to this point shows the potential of using CMC to enhance the controlled release behaviour of the Zn/Al-LDH nanocomposite.

Kinetic Study of QC from the Zn/Al-LDH-QC-CMC Nanocomposite into Various Aqueous Solution

To obtain further details concerning the release mechanism of the intercalated QC, the release data from the release study in the aqueous solutions of Na_3PO_4, Na_2SO_4, and NaCl were fitted to several kinetic models, as plotted in Fig. 9, Fig. 10, and Fig. 11, respectively. Five types of kinetic models were chosen to be fitted in the study, which are zeroth order (Eq. (1)), first order (Eq. (2)) [72], pseudo-second order (Eq. (3)) [73], parabolic diffusion (Eq. (4)) [74], and Fickian diffusion models (Eq. (5)) [75].

$$x = t + c \tag{1}$$

$$-\log(1 - M_i/M_f) = t + c \tag{2}$$

Table 3 Comparison of the percentage release of QC from Zn/Al–LDH–QC, Zn/Al–LDH–QC–Chi and Zn/Al–LDH–QC–CMC into single, binary and ternary aqueous systems of phosphate, sulphate and chloride

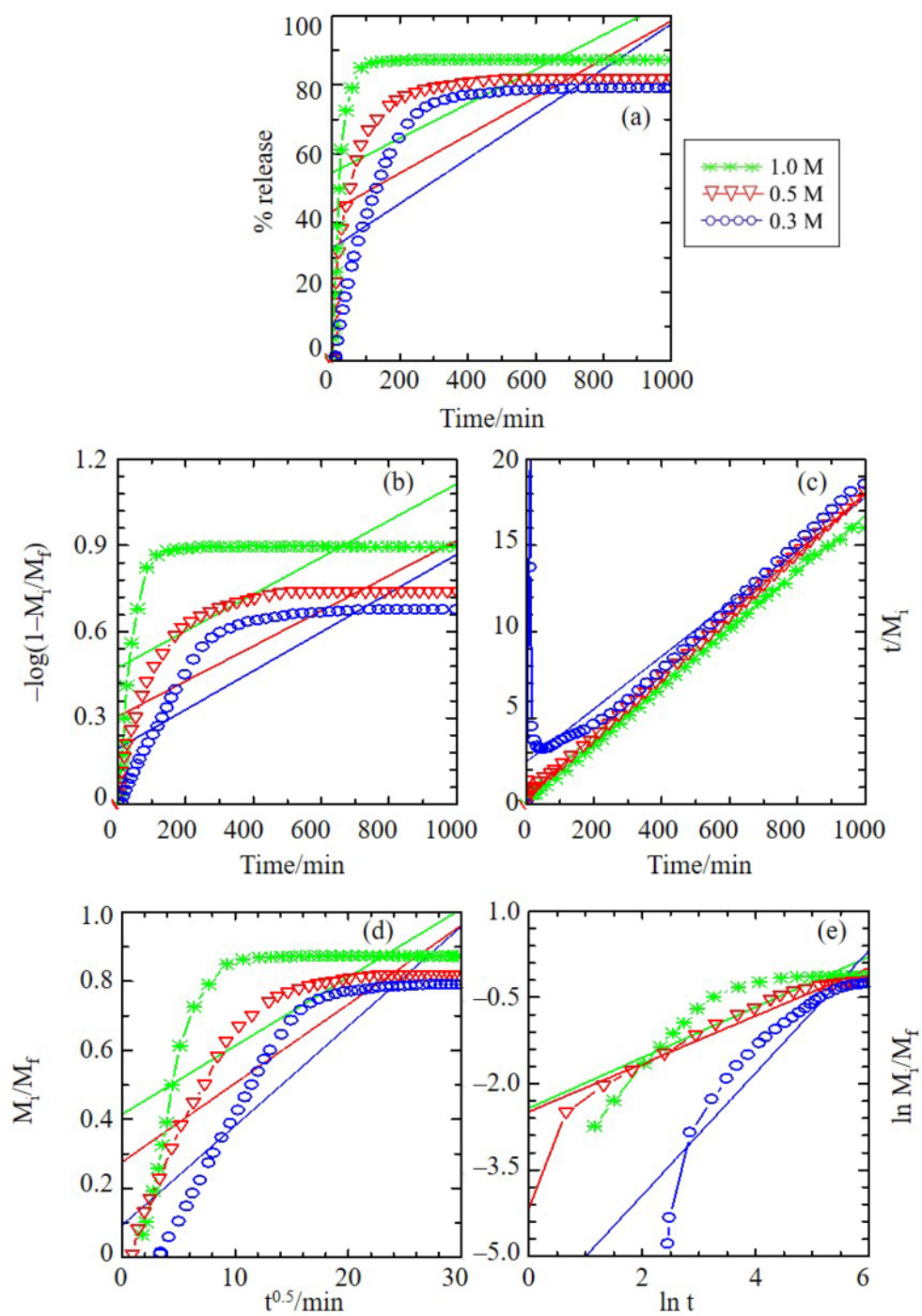| Aqueous solutions			Zn/Al–LDH–QC		Zn/Al–LDH–QC-Chi		Zn/Al–LDH–QC–CMC	
			Percentage release (%)	Release time (min)	Percentage release (%)	Release time (min)	Percentage release (%)	Release time (min)
Single	PO_4^{3-}	0.3 M	73.9	356	70.3	608	78.9	614
		0.5 M	80.5	221	75.7	265	81.8	480
		1.0 M	81.2	99	80.8	103	87.3	163
	SO_4^{2-}	0.3 M	47.2	1161	68.1	1255	22.4	1436
		0.5 M	77.0	714	74.6	1192	31.7	1259
		1.0 M	81.8	84	78.2	112	70.1	245
	Cl^-	0.3 M	73.8	2639	62.0	3176	78.4	6083
		0.5 M	76.0	2168	63.4	2855	79.3	4506
		1.0 M	82.4	693	74.4	1646	80.0	3004
Binary	$PO_4^{3-} - SO_4^{2-}$		79.2	329	70.6	611	72.5	1498
	$PO_4^{3-} - Cl^-$		77.5	1015	70.0	1045	55.1	1618
	$SO_4^{2-} - Cl^-$		75.6	1359	73.3	1436	42.0	2518
Ternary	$PO_4^{3-} - SO_4^{2-} - Cl^-$		80.3	138	73.8	269	83.5	277
Ref			[54]		[54]		Present paper	

Fig. 9 Fitting of the data for QC release from Zn/Al–LDH–QC–CMC into aqueous solution of sodium phosphate for the **a** zero order, **b** first order, **c** pseudo second order, **d** parabolic diffusion and **e** Fickian diffusion kinetic models
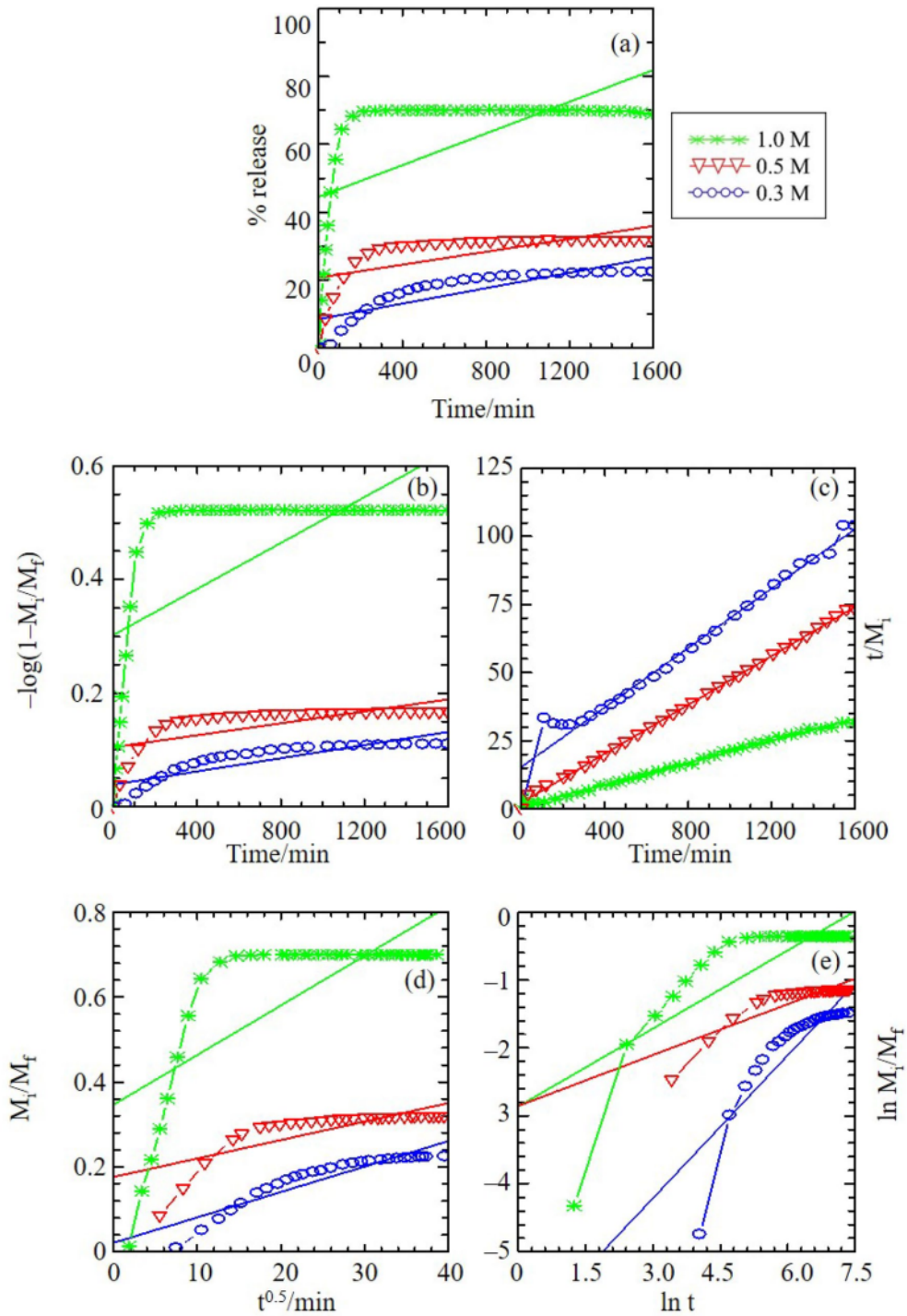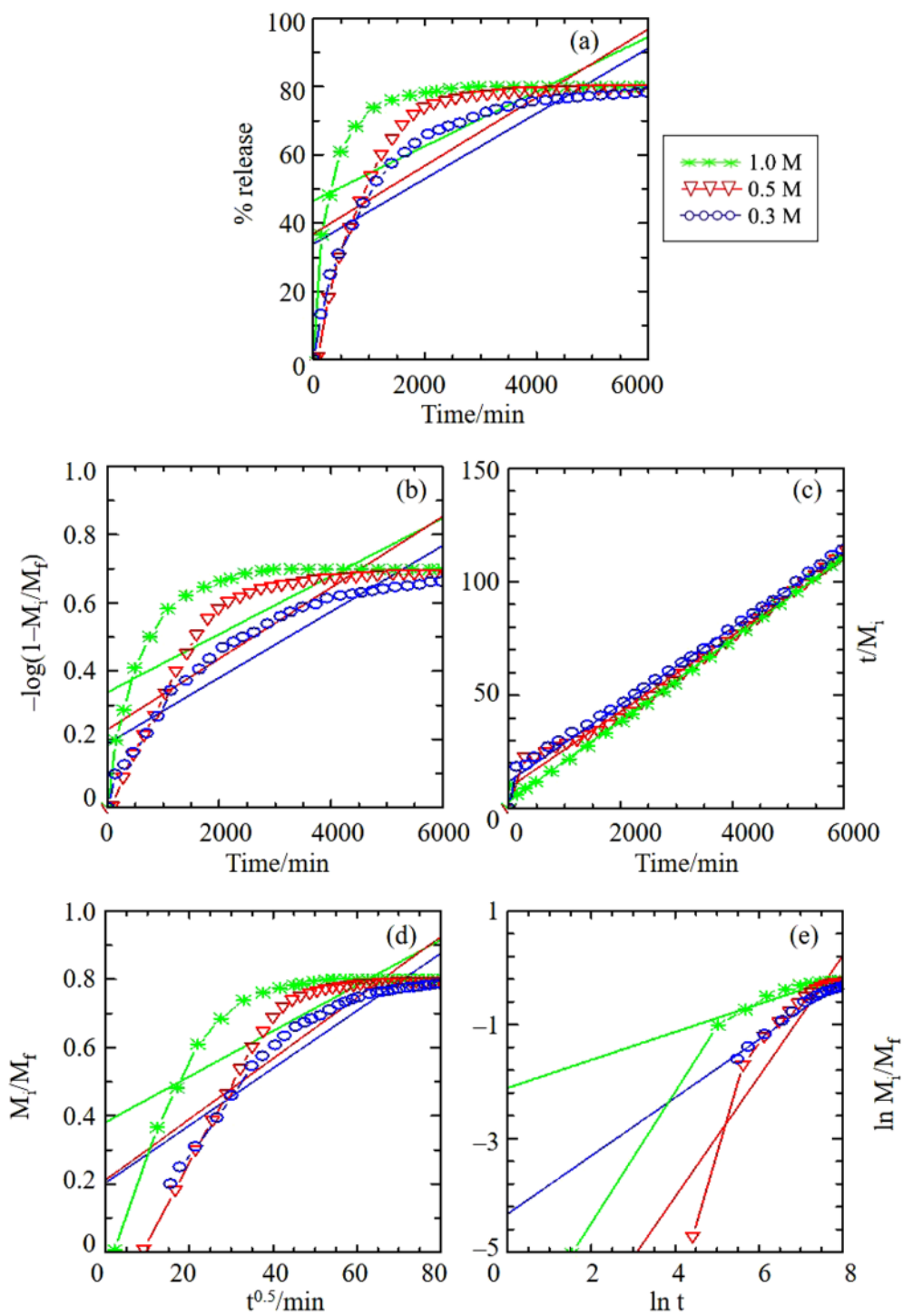
Fig. 10 Fitting of the data for QC release from Zn/Al–LDH–QC–CMC into aqueous solution of sodium sulphate for the **a** zero order, **b** first order, **c** pseudo second order, **d** parabolic diffusion and **e** Fickian diffusion kinetic models

Fig. 11 Fitting of the data for QC release from Zn/Al–LDH–QC–CMC into aqueous solution of sodium chloride for the **a** zero order, **b** first order, **c** pseudo second order, **d** parabolic diffusion and **e** Fickian diffusion kinetic models

$$t/M_i = 1/M_f^2 + t/M_f \qquad (3)$$

$$M_i + M_f = kt^{0.5} + c \qquad (4)$$

$$M_i + M_f = kt^n \qquad (5)$$

In the provided equations, x is the percentage release of QC from the Zn/Al-LDH-QC-CMC nanocomposite at time t, c is the constant, and M_i and M_f represent the initial and final concentration of the QC, respectively.

The rate constant, k, is calculated according to the equation of the kinetic model, the halftime, $t_{1/2}$ is the half of the time taken for the release of the intercalated QC to reach equilibrium and the regression values, r^2 were determined by fitting the release data into the previously mentioned kinetic models; the value nearest to 1 was selected as the best fit. The values of k, $t_{1/2}$, and r^2 obtained from the release data of the Zn/Al-LDH-QC-CMC nanocomposite in each release media are summarised in Table 4.

The comparison made on the $t_{1/2}$ values in Table 4 shows that the release of the Zn/Al-LDH-QC-CMC nanocomposite that was carried out in NaCl has the highest $t_{1/2}$ values, in the order of $Cl^- > SO_4^{2-} > PO_4^{3-}$. This sequence indicates that the $t_{1/2}$ values were greatly influenced by the charge density of the anions in the released media. The $t_{1/2}$ values also increase when the release was performed in a higher concentration of release media, as more anions were provided in the release media of higher concentration [76].

Of all the present models, the pseudo-second order one gave the best r^2 values, which range 0.878–1.000. The linearization of the release data into other kinetic models used in the study only led to poorer r^2 values. Hence, this indicates that the release of the QC from the Zn/Al-LDH-QC-CMC nanocomposite in all release media is best described by the pseudo-second-order kinetic model. This reveals

that the mechanism of the release process of the intercalated QC into the release media took place via dissolution of the nanocomposite and the ion exchange between QC and the anions that can be found in the release media [76].

The ability of CMC to prolong the release time is triggered by its hygroscopic nature and swellable properties that allowed the CMC to the form gel layer when immersed in liquid system [27, 77–79]. The development of the gel layer that encloses the Zn/Al-LDH-QC-CMC nanocomposite can be divided into three distinguishable regions [80]. The outermost region of the gel layer, which is called the 'erosion front' is highly swollen and contain the highest amount of water molecule, although it is mechanically weak. This region acts as a diffusion barrier that assists in preventing water penetration into the inner regions. The middle region, which also known as the 'dissolution front' is averagely swollen and possesses better mechanical strength than the erosion front. The presence of both the erosion front and the dissolution front keeps the innermost region of the gel layer, the 'swelling front', to be essentially dry, thus allowing it to hold its glassy state for an extensive period.

When the Zn/Al-LDH-QC-CMC were exposed in the release media, more water penetrated into the CMC matrix, causing the gel layer formed to be hydrated and swelled, thus initiate the erosion of the CMC surface. The swelling will start from the outermost region, and followed by the middle region and the innermost region, as the outermost region will be hydrated faster compare to the inner region. The slow dissolution of the CMC surface slowed the rate of ion exchange between the intercalated QC and the anions in the release media. The hydration induces the polymeric chain of the CMC to undergo chain relaxation (which is signified by the swelling), and results in the disentanglement of the polymeric chain [80]; the CMC matrix then gradually disappears.

Table 4 Comparison of rate constants (k), regression values (r^2) and half-life ($t_{1/2}$) obtained from the fitting of the release data from Zn/Al–LDH–QC–CMC into aqueous solutions of Na₃PO₄, Na₂SO₄ and NaCl

Aqueous solution		Zeroth order	First order	Parabolic diffusion	Fickian diffusion	Pseudo-second order		
		r^2	r^2	r^2	r^2	r^2	k ($\times 10^{-3}$ s^{-1})	$t_{1/2}$
Na₃PO₄	0.3 M	0627	0.735	0.832	0.860	0.878	0.158	93.7
	0.5 M	0.516	0.634	0.754	0.958	0.999	0.477	31.2
	1.0 M	0.380	0.448	0.578	0.803	0.999	0.845	17.6
Na₂SO₄	0.3 M	0.711	0.739	0.861	0.767	0.974	0.066	224.1
	0.5 M	0.420	0.440	0.608	0.751	0.999	0.199	74.9
	1.0 M	0.367	0.414	0.561	0.653	0.996	0.381	39.0
NaCl	0.3 M	0.716	0.860	0.875	0.981	0.993	0.021	717.1
	0.5 M	0.602	0.725	0.744	0.839	0.988	0.023	662.4
	1.0 M	0.439	0.559	0.619	0.910	0.997	0.087	170.7

Conclusion

This study proposes a new class of herbicides that are greener, safer, and more environmentally friendly. The characterisation study shows that the CMC coating process did not cause any alteration on the type of anion intercalated in the interlayer gallery of Zn/Al-LDH. In fact, the CRF applied in the Zn/Al-LDH-QC using CMC as the coating material was proven to prolong the time of the release of the intercalated QC, thereby reducing the risk of environmental pollution typically caused by the excessive use of pesticides. The kinetic studies conducted using the obtained release data showed that the release behaviour of QC from the Zn/Al-LDH-QC-CMC nanocomposite follows the pseudo-second-order model. The fabrication of such nanomaterials gives the possibility towards finding a solution to reduce the rate of high diffusion of chemicals into soils. Hence, assist in lessening the environmental issues triggered by the excessive herbicide residues.

Compliance with Ethical Standards

Conflict of interest The authors declare that they have no conflict of interest.

References

1. Fernández-Pérez M, Villafranca-Sánchez M, Flores-Céspedes F, Daza-Fernández I (2011) Carbohydr Polym 83:1672–1679
2. Céspedes FF, García SP, Sánchez MV, Pérez MF (2013) Chemosphere 92:918–924
3. Grillo R, Dos Santos NZP, Maruyama CR et al (2012) J Hazard Mater 231–232:1–9
4. Bashi AM, Hussein MZ, Zainal Z et al (2016) Arab J Chem 9:1457–1463
5. Nejati K, Davary S, Saati M (2013) Appl Surf Sci 280:67–73
6. Touloupakis E, Margelou A, Ghanotakis DF (2011) Pest Manag Sci 67:837–841
7. Sarijo SH, Ghazali SAI SM, Hussein MZ, Ahmad AH (2015) Mater Today Proc 2:345–354
8. Liu J, Zhang X, Zhang Y (2015) ACS Appl Mater Interfaces 7:11180–11188
9. Isa IM, Sharif SNM, Hashim N, Ghani SA (2015) Ionics (Kiel) 21:2949–2958
10. Isa IM, Dahlan SNA, Hashim N et al (2012) Int J Electrochem Sci 7:7797–7808
11. Wardani NI, Isa IM, Hashim N, Ghani SA (2014) Sens Actuator B Chem 198:243–248
12. Zainul R, Azis NA, Isa IM et al (2019) Sensors 19:941
13. Aziz INFA, Sarijo SH, Rajidi FSM et al (2019) J Porous Mater 26:717–722
14. Ahmad MS, Isa IM, Hashim N et al (2018) J Solid State Electrochem 22:2691–2701
15. Garrido J, Cagide F, Melle-Franco M et al (2014) J Mol Struct 1061:76–81
16. Huang Y, Hu Q, Cui G et al (2020) J Environ Sci Health - Part B 55:342–354
17. Al-Kahtani AA, Sherigara BS (2014) Carbohydr Polym 104:151–157
18. Feng S, Wang J, Zhang L et al (2020) Geofluids 20:1–16
19. Li GB, Wang J, Kong XP (2020) Carbohydr Polym 249:116865
20. Chenxi Y, Juan L, Jian W et al (2020). New J Chem. https://doi.org/10.1039/d0nj02771e
21. Cozzolino CA, Nilsson F, Iotti M et al (2013) Colloids Surf B Biointerfaces 110:208–216
22. Lavoine N, Desloges I, Bras J (2014) Carbohydr Polym 103:528–537
23. Lavoine N, Tabary N, Desloges I et al (2014) Colloids Surf B Biointerfaces 121:196–205
24. Teng Z, Luo Y, Wang Q (2013) Food Chem 141:524–532
25. Teixeira MA, Paterson WJ, Dunn EJ et al (1990) Ind Eng Chem Res 29:1205–1209
26. Azevedo MA, Bourbon AI, Vicente AA, Cerqueira MA (2014) Int J Biol Macromol 71:141–146
27. Serrano-Cruz MR, Villanueva-Carvajal A, Morales Rosales EJ et al (2013) LWT-Food Sci Technol 50:554–561
28. Mahkam M, Davatgar M, Rezvani Z, Nejati K (2013) Int J Polym Mater Polym Biomater 62:57–60
29. Yadollahi M, Namazi H, Barkhordari S (2014) Carbohydr Polym 108:83–90
30. Shu Y, Bai Q, Fu G et al (2020) Carbohydr Polym 227:115346
31. Pirsa S, Farshchi E, Roufegarinejad L (2020). J Polym Environ. https://doi.org/10.1007/s10924-020-01846-0
32. Xu W, Li Z, Shi S et al (2020) Appl Catal B Environ 262:1–806
33. Duan Y, Tan J, Huang Z et al (2020) Carbohydr Polym 249:116882
34. Roy S, Rhim JW (2020) Int J Biol Macromol 148:666–676
35. Bhatti HN, Safa Y, Yakout SM et al (2020) Int J Biol Macromol 150:861–870
36. Wang F, Zhang Q, Huang K et al (2020) Int J Biol Macromol 154:1392–1399
37. Hao M, Gao P, Yang D et al (2020) Environ Pollut 267:114142
38. Nakagawa K, Sowasod N, Tanthapanichakoon W, Charinpanitkul T (2013) LWT - Food Sci Technol 54:600–605
39. Li J, Li Y, Dong H (2008) J Agric Food Chem 56:1336–1342
40. Sharif SNM, Hashim N, Md Isa I et al (2018) Mater Res Innov 23:260–265
41. Yadav M, Rhee KY, Jung IH, Park SJ (2013) Cellulose 20:687–698
42. Hussein MZ, Hashim N, Yahaya A, Zainal Z (2011) Sains Malaysiana 40:887–896
43. Kura AUU, Hussein-Al-Ali SHH, Hussein MZZ et al (2014). Sci World J. https://doi.org/10.1155/2014/104246
44. Feng Y, Li D, Wang Y et al (2006) Polym Degrad Stab 91:789–794
45. He FA, Zhang LM, Yang F et al (2006) J Polym Res 13:483–493
46. Costantino U, Gallipoli A, Nocchetti M et al (2005) Polym Degrad Stab 90:586–590
47. Li B, He J, Evans DG (2008) Chem Eng J 144:124–137
48. Rives V, Ulibarri MA (1999) Coord Chem Rev 181:61–120
49. Taibi M, Ammar S, Jouini N et al (2002) J Mater Chem 12:3238–3244
50. Hussein MZ, Jaafar AM, Yahaya AH, Zainal Z (2009) Nanoscale Res Lett 4:1351–1357
51. Babakhani S, Talib ZA, Hussein MZ, et al. (2014) https://doi.org/10.1155/2014/467064
52. Angadi SC, Manjeshwar LS, Aminabhavi TM (2010) Int J Biol Macromol 47:171–179

53. Fernandez JM, Ulibarri MA, Labajos FM, Rives V (1998) J Mater Chem 8:2507–2514
54. Sharif SNM, Hashim N, Isa IM et al (2020). Mater Chem Phys. https://doi.org/10.1016/j.matchemphys.2020.123076
55. Dorniani D, Hussein MZ, Kura AU et al (2013) Int J Mol Sci 14:23639–23653
56. Xu W, Di C, Zhou S et al (2015) Front Genet 6:1–15
57. Pareja L, Pérez-Parada A, Agüera A et al (2012) Chemosphere 87:838–844
58. Liang X, Jin Y, He M et al (2017) Agric Ecosyst Environ 237:173–180
59. Zhang A, Chen Z, Zhang G et al (2012) Eur J Soil Biol 52:73–77
60. Bond JA, Walker TW (2012) Weed Technol 26:183–188
61. Sudianto E, Beng-Kah S, Ting-Xiang N et al (2013) Crop Prot 49:40–51
62. Rodenburg J, Demont M (2009) AgBioForum 12:313–325
63. Jiangzhou HE (2008) Dong QU 20:1103–1108
64. Cho JY, Nishiyama M, Matsumoto S (2002) Soil Sci Plant Nutr 48:461–468
65. Ducloux J, Guero Y, Fallavier P, Valet S (1994) Geoderma 64:57–71
66. Nguyen MN, Dultz S, Kasbohm J, Le D (2009) J Plant Nutr Soil Sci 172:477–486
67. Sun H, Xia L, Liang S, Shen S (2014) Food Anal Methods 7:1791–1797
68. Ghazali SAI SM, Hussein MZ, Sarijo SH (2013) Nanoscale Res Lett 8:1–8
69. Li S, Shen Y, Xiao M et al (2015) Arab J Chem 12:2563–2571
70. Hussein MZ, Hashim N, Yahaya AH, Zainal Z (2009) J Nanosci Nanotechnol 9:2140–2147
71. Emeje MO, Kunle OO, Ofoefule SI (2006) Acta Pharm 56:325–335
72. Hussein MZ, Rahman NSSA, Sarijo SH, Zainal Z (2012) Appl Clay Sci 58:60–66
73. Ho YS, Mckay G (1999) Process Biochem 34:451–465
74. Kodama T, Harada Y, Ueda M et al (2001) Langmuir 17:4881–4886
75. Ritger PL, Peppas NA (1987) J Control release 5:37–42
76. Hashim N, Muda Z, Hamid SA et al (2014) J Phys Chem Sci 1:1–6
77. Hao L, Lin G, Lian J et al (2020) Carbohydr Polym 231:115725
78. Chen L, Zhou H, Hao L et al (2020) Ind Crops Prod 150:112358
79. Pooresmaeil M, Behzadi Nia S, Namazi H (2019) Int J Biol Macromol 139:994–1001
80. Woo MA, Kim TW, Paek MJ et al (2011) J Solid State Chem 184:171–176

Polymeric Nanocomposite‑Based Herbicide of Carboxymethyl Cellulose Coated‑Zinc/Aluminium Layered Double Hydroxide‑Quinclorac: A Controlled Release Purpose for Agrochemicals

efficient and selective adsorption of In 3+ on pristine Zn/Al layered double hydroxide (Zn/Al-LDH) from aqueous solutions", Journal of Solid State Chemistry, 2016

Exclude quotes   On

Exclude bibliography   On

Exclude matches   < 100 words